energies

Article

Effects of an Exhaust System Equipped with a Thermoelectric Generator on Combustion, Performance, Emissions, and Energy Recovery in a Diesel Engine Using Biodiesel

Murat Karabulut [1], Cenk Sayın [1] and Sinan Erdoğan [2,*]

[1] Department of Mechanical Engineering, Marmara University, 34722 Istanbul, Türkiye; mkarabulut@marun.edu.tr (M.K.); csayin@marmara.edu.tr (C.S.)
[2] Mechatronics Program, Adapazari Vocational School, Sakarya University, 54050 Sakarya, Türkiye
* Correspondence: sinanerdogan@sakarya.edu.tr

Abstract: The predominance of petroleum-based fuels is lessened by the preference for biodiesel as an alternative. However, one of the adverse effects arising from the use of biodiesel is the formation of waste heat. The novel aspect of this study proposes a sustainable solution that will decelerate global warming by recovering waste heat through a new exhaust design equipped with thermoelectric generators. The study obtained test fuels by blending vegetable-derived biodiesel in five different volumetric ratios (0, 10%, 20%, 50%, and 100%). The experiments were carried out at three different constant engine speeds (1000, 1250, and 1500 RPM) and five different engine loads (25%, 50%, 75%, and 100%) on a single-cylinder diesel engine. At the end of the experiment, the combustion characteristics, engine performance, exhaust emissions, waste heat values, and electrical energy gained from the thermoelectric system of biodiesel blend fuels compared to diesel were evaluated. Specific fuel consumption, effective efficiency, exhaust gas temperatures, exhaust emissions, and electrical power generation with TEG in the diesel engine were evaluated, focusing on the different biodiesel blend ratios, engine load, and engine speeds.

Keywords: thermoelectric generator; biodiesel; emission; diesel engine; waste heat recovery

Citation: Karabulut, M.; Sayın, C.; Erdoğan, S. Effects of an Exhaust System Equipped with a Thermoelectric Generator on Combustion, Performance, Emissions, and Energy Recovery in a Diesel Engine Using Biodiesel. *Energies* **2024**, *17*, 1083. https://doi.org/10.3390/en17051083

Academic Editors: Mahmoud Bourouis, Nadjet Zioui, Peter Breuhaus and Said Bentouba

Received: 30 January 2024
Revised: 20 February 2024
Accepted: 22 February 2024
Published: 24 February 2024

1. Introduction

Energy is supplied by petroleum products for ICEs, which are frequently used in transportation and power generation. Researchers have focused on the use of alternative energy sources, as well as improving fuel savings and decreasing emissions, due to the scarcity of energy resources, the global crises, and environmental factors. Biodiesel fuels derived from vegetable and animal fats are alternative fuels that can replace petroleum-based fuels. Biodiesel fuels also provide advantages over petroleum-based fuels in terms of emission values [1].

ICEs are one of the leading sources of air pollution. Exhaust emissions from ICEs mainly contain nitrogen oxides (NO_x), carbon monoxide (CO) unburned hydrocarbons (HC), particulate matter (PM), sulfur oxides (SO_x), and lead (Pb). These pollutant emissions have harmful and dangerous effects on human health, animals, and the environment. For this reason, countries are taking measures and developing standards to restrict exhaust emissions in international authorities and forcing manufacturers in the automotive sector to comply with these standards.

Over 60% of the fuel energy distribution in a light-duty vehicle, operating over a typical city drive cycle, is lost through the thermal engine [2]. While most of the research in recent years aimed to prevent waste heat, other research aimed to recover waste heat. The waste heat from the exhaust system of the ICE can be recovered and converted to electrical energy through thermoelectric generators (TEGs) [3,4]. Therefore, the use of TEG systems gains importance in terms of environmental sustainability.

The intensive recent studies on systems with TEGs' ability to generate electricity from waste heat were conducted due to these systems' ability to produce energy across a wide thermal range. With systems that can assist the alternator system, or be used instead of the alternator, there may be decreases in fuel consumption and emissions. TEGs are a promising technology for the automotive industry in terms of their low maintenance costs, small footprint, quiet and vibration-free operation, and the direct usability of the electricity they produce. However, a low energy efficiency is among their disadvantages [4].

Apart from the waste heat recovery, another environmentally sensitive field of study is the use of alternative fuels instead of petroleum-derived fuels. Emissions from engines using alternative fuels are generally cleaner than emissions from diesel and gasoline engines [5,6]. The Euro 6 emission regulation aims to reduce the environmental pollution caused by exhaust gases. However, there is a disadvantage to the use of biodiesel. Due to its high oxygen content, biodiesel increases the amount of NO_x emissions, which is a natural result of the reaction. For this, additional measures need to be taken [7].

When the literature studies with ICE were analyzed, experimental studies on the use of alternative fuels, such as biodiesel, ethanol, and methanol, were encountered. Some of these studies are as follows:

- Soyler [8] conducted tests on a single-cylinder diesel engine with the biodiesel produced from waste olive oil. The produced biodiesel was blended at six different volumetric ratios (0, 20%, 40%, 60%, 80%, and 100%) and the tests were carried out at a constant engine speed of 1500 RPM and four different engine loads (25%, 50%, 75% and 100%). Each fuel was tested at four different injection pressures (from −100 to +200 bar) and four different injection timings (−2°–+4° crank angle). As a result, the specific fuel consumption increased and the maximum cylinder pressure, nitrogen monoxide, and carbon dioxide emissions decreased, with an increase in the biodiesel content in the mixture. When the mixture ratio exceeded 40%, engine power began to decrease. Reducing the injection timing caused a decrease in engine power, NO, and CO_2 emissions, but an increase in specific fuel consumption and HC emissions. In addition, reducing the pressure decreased CO_2 and NO emissions but increased HC emissions.
- Leevijit and Prateepchaikul [9] blended biodiesel derived from palm oil at three different volumetric ratios in their study. The blended fuels were burned in a four-cylinder diesel engine under different loads (5–37.5 kW) and at a constant engine speed of 2400 RPM. The engine performance and exhaust emission values that were obtained were compared with diesel. As a result, it was observed that the specific fuel consumption values of the blended fuels (20%, 30%, and 40%) were 4.3%, 5.9%, and 7.6% higher than diesel and the thermal efficiencies were 3%, 4.1% and 5.2% lower than diesel, respectively. The smoke emissions of all blended fuels were significantly lower and the NO_x emissions were higher than diesel.
- Sanjid et al. [10] conducted an experimental study in a four-cylinder, water-cooled, 2.5 L diesel engine at different speeds between 1000 and 4000 RPM with different mixing ratios of biodiesel produced from mustard oil and palm oil, and the engine performance and exhaust emission values were compared with those of diesel. As a result, the specific fuel consumption of blended fuels appeared higher than those of diesel, the maximum engine power of mustard oil biodiesel blends was lower than that of diesel, and the maximum and average power outputs of palm oil biodiesel blends were almost the same compared to diesel. All blended fuels were found to have lower HC and CO emissions and higher NO emissions than diesel.

Among the studies on biodiesel, no studies on the use of TEG were found. Examples of some studies in the literature on the combined use of TEG systems with diesel or gasoline fuels are given below.

- Niu et al. [11] designed and mathematically modeled a three-dimensional exhaust system with thermoelectric modules to recover waste thermal energy from the exhaust system. The input parameters of the model are based on the data of a six-cylinder internal combustion diesel engine at 1500 RPM constant speed at four different engine loads. In the experiments, 13.1–23.9 W of electrical power was obtained from the TEG system. The efficiency of the TEG modules was calculated as 4%.

- Liu et al. [12] used a two-stage thermoelectric model and designed a 100 mm straight pipe with 96 Bi_2Te_3-based modules arranged in coils around the exhaust pipe and passing through the center. According to the theoretical and experimental results, the highest power was obtained with a temperature difference of 175 K at the optimum point, and 202 W of the maximum electrical power was measured. As a result of the study, it was observed that the thermal efficiency increased by 5.35%.
- Orr et al. [13] aimed to reduce CO_2 emissions and operating costs with a thermoelectric generator consisting of eight parallel connected modules integrated into the exhaust system of a vehicle's ICE with a 3.0 L V6 engine. In the study, the maximum power output of the system for all tests was 38 W from the eight 62 mm × 62 mm TEGs that were used. The rate of heat transfer in this case was 1541 W, with the TEG efficiency of 2.46%.
- Lan et al. [14] designed a waste gas recovery model using 20 TEG modules. They applied the model to a commercial diesel engine. The thermoelectric generator modules were placed in the exhaust gas recycling valve (EGR) line. The system is cooled by a chiller. An electrical power of 170–224 W was obtained from 20 TEG modules. As a result of the installed system, 25.8% of the waste energy was recovered.
- Fernández-Yáñez et al. [15] used two types of engines, spark-ignition (SI) and compression-ignition (CI), in their study. The study aimed to determine the values of electricity generation and pressure drop losses under boundary conditions. After TEG modules made of commercially available Bi_2Te_3 material were added to the system, measurements were taken again. Both engines were tested for electricity generation under full load conditions. A potential fuel saving of 0.56% was achieved in the gasoline engine, and 1.09% in the diesel engine. The highest electrical power obtained during the tests was 270 W.
- Kim et al. [4] conducted the tests at the ICE with a four-stroke, four-cylinder, 2 L hybrid vehicle in nine different operating modes and evaluated the results. In the study, a recovery system was built from 12 TEG modules. The system is cooled using the engine's cooling system. The maximum electrical power output of the system is 118 W, and the thermal efficiency is 2.1%.
- Dinçer and Ezzat [16] used a Bi_2Te_3-based thermoelectric generator integrated into an ICE with a volume of 2.3 L, running on ammoniumnitrate-derived hydrogen. In the experimental study, a maximum power output of 4 W was obtained with a temperature difference of 250 °C.
- Ziolkowski [17] placed thermoelectric generators in two separate engines: a 1.2 L twin-charged direct injection petrol engine and a 1.3 L small diesel engine. The 24 Bi_2Te_3-based TEG modules used in the study were placed in a rectangular arrangement around a rectangular heat exchanger. The efficiency of the TEG modules that were used is in the range of 0.14–1.6%. When these modules were applied to engines, the heat recovery efficiency did not exceed 0.29% in petrol engines and 0.27% in diesel engines.
- In a study, Uysal [18] mounted a circular-shaped thermoelectric generator consisting of 96 pairs of p-type and n-type thermoelectric legs in the exhaust system of a four-cylinder diesel engine. In the study, p-type $Ca_{2.5}Ag_{0.3}Eu_{0.2}Co_4O_9$ thermoelectric materials resistant to 900 °C and n-type $Zn_{0.96}Al_{0.02}Ga_{0.02}O$ thermoelectric materials resistant to 1350 °C were produced and their thermoelectric properties were measured. The generator was tested by connecting the TEGs just in front of the exhaust silencer of the diesel engine. The TEG was cooled with mains water. In the thermoelectric module, a voltage of 278 mV was obtained at a temperature difference of 203 °C. The circular TEG that was produced was able to produce 30% of the theoretical voltage. The main reason for this is the high internal resistance of the produced circular TEG.

- Temizer [19], in his study, aimed to recover energy waste thermal energy by placing a heat exchanger and TEG in the exhaust system. In the system, 40 Bi_2Te_3-based TEG modules were used and electrically connected in series among themselves. The octagonal geometry consists of a group of five modules, lined horizontally on each surface. In the experiments, a four-cylinder, four-stroke, Turbocharged Common Rail 1.9 L Fiat Doblo diesel engine was used. The engine was operated at 1500, 2000, 2500, 3000, and 3500 RPM at three different load values of 50, 75, and 100 Nm, respectively. As a result, exhaust gas temperatures ranging from 110 to 320 °C were obtained. As a result of the experiment, a voltage in the range of 13–60 V, and in the range of 1500–3500 RPM at 50 Nm loading, was measured in the TEG system. The calculated power value varies between 8.58 and 140.6 W. At a full load, 156.7 W power output was measured as the maximum power value.
- Güneş and Hançer [20] converted the waste thermal energy on the exhaust pipe using TEG modules. The TEG is cooled by a heat exchanger structure using a variable conductivity heat pipe. The optimum operating temperature of the heat pipes used in the study was found to be 150 °C. A power of 38 W was obtained at the optimum operating temperature.
- Mohammed [21] placed thirty thermoelectric modules (five on each side and twenty on the bottom) on the exhaust pipe of a diesel engine. The current values and power values were measured in the range of 750–3750 RPM from the TEG system. In the study, a 340 °C exhaust gas temperature was reached at 3750 RPM, and 214 W maximum electrical power was obtained. According to the study, 62 W of electrical power was obtained via urban use and 212 W of the electrical power was obtained via non-urban use. The efficiency of the TEG system was calculated as 4.63%.
- Remeli et al. [22] measured 0.85 A and 2.02 V at a temperature difference of 95 °C between the two faces of the TEG. The maximum generated electrical power was calculated as 7 W and was stated to be 16% less than the theoretical calculation.
- Hsu et al. [23] placed 24 thermoelectric modules around the channel through which the hot gas passed in their study. In the experiments, 12.41 W power was produced with 0.64 A when the temperature difference was 30 K.
- In et al. [24] used a total of twenty thermoelectric modules, ten HZ-20 and ten HZ-14, in the exhaust of a 2.2 L diesel engine. The heat exchanger design was made square around the exhaust pipe and five TEGs were placed on each face of the square design. An average of 6.2 W and 3.6 A was measured when the temperature was 170 °C.
- In another study, Kim et al. [25] experimentally examined the exhaust heat exchanger they designed to produce electricity from waste heat using 40 TEGs. A six-cylinder diesel engine was used as the heat source and was operated at three different speeds: 1000, 1500, and 2000 RPM. The maximum power was obtained at 2000 RPM with 119 W at a temperature difference of 304 K.
- Orr et al. [13] used eight TEG modules in their study on the recovery of waste heat in the exhaust of a 3.0 L V6 engine. The first experiment was carried out with the engine running at 2500 RPM and with no load, while the device was horizontal. Under these conditions, 15.17 W power was produced at a temperature difference of 187 °C. In the second experiment, 37.85 W power was produced when the engine was at 4000 RPM and with no load, while there was a temperature difference of 271 °C.
- Kim et al. [26] examined the heat recovery characteristics of a direct-contact TEG in their experimental study, in which 40 modules made of Bi_2Te_3 material were used. The system was mounted on the exhaust of the engine operating in the range of 1700–2300 RPM and generated approximately 12–45 W power with a TEG efficiency of 1–2%.
- Mostafavi and Mahmoudi [27] used a total of eight TEG modules (TEC 12706) in their experiments. The temperature difference between the hot and cold module surfaces was 20, 45, 70, 95, and 120 °C; approximately 0.2, 0.4, 1.0, 2.0, and 3.5 W output power was obtained.

The use of biodiesel aims to reduce harmful gas emissions. However, although this fuel helps to prevent environmental pollution and create a sustainable future, it does not provide a solution to global warming. Using biodiesel in ICE will create waste heat as a result of combustion.

The exhaust temperatures can be as high as 900 °C for spark-ignition (SI) engines and around 500 °C for compression-ignition (CI) engines [2]. During the discharge of gases from the exhaust, a very high rate of heat transfer occurs, and the gas temperature drops to 200 °C. However, there is a significant difference in temperature between a standard air temperature of 25 °C and the exhaust gas temperatures. This temperature difference can be converted into electrical energy using TEG systems.

What makes this study different from others is that it reduces the high temperature of the exhaust gases formed using biodiesel, which causes global warming. In this way, waste heat can be recovered and the exhaust gases can be released into the environment at lower temperatures.

This study aims to reduce exhaust emissions by using alternative fuel and recover waste thermal energy by using a new exhaust system with TEG. In addition, an experimental study on recovering waste heat energy through a TEG system in an ICE, using biodiesel as fuel, has been included in the literature.

2. Materials and Methods

The experimental study was carried out in the test unit located in The Scientific and Technological Research Council of Türkiye–Rail Transport Technologies Institute (TÜBİTAK-RUTE). The test unit consists of a single-cylinder, four-stroke diesel experimental engine, Eddy current dynamometer, emission measurement device, air and fuel measurement device, and in-cylinder pressure measurement system. A schematic view of the experimental setup is presented in Figure 1.

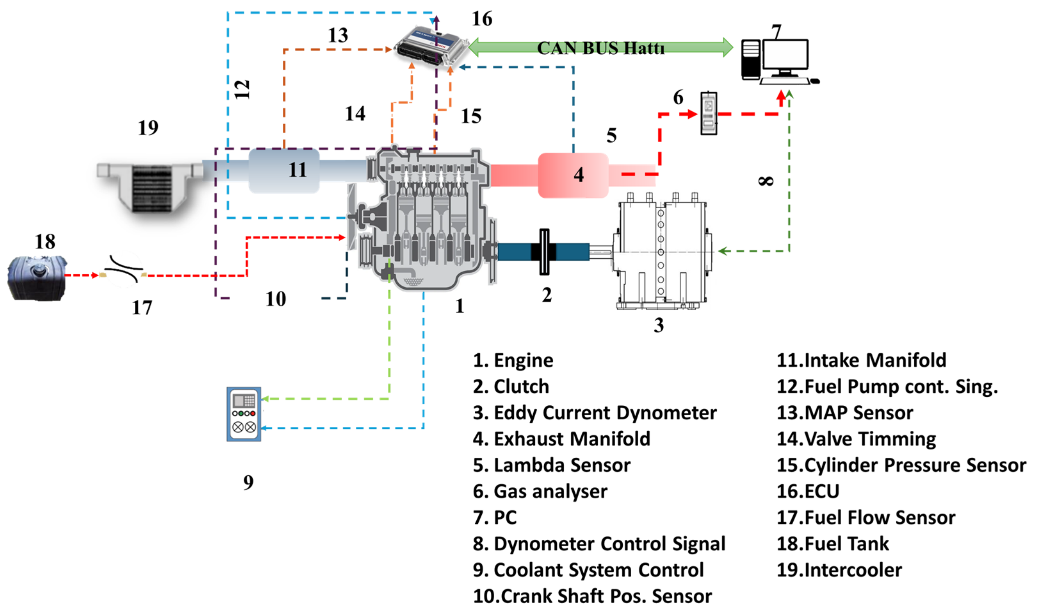

Figure 1. Schematic view of the experimental setup.

Engine loading in the test unit was provided by a dynamometer connected to the crankshaft. The room where the test engine was located was an air-conditioned environment with a standard conditioned temperature of 25 °C at a pressure of 1 atm. Engine cooling water, engine oil, and fuel temperature were prepared by the system to suit the operating conditions. In addition to the engine test unit, a separate emission measurement device was used for emission measurement. All measurements and parameters in the test environment were recorded by the computer connected to the test unit.

2.1. Characteristics of Diesel Engine

The experimental study was performed using a single-cylinder, water-cooled, four-strokes, and turbo-direct-injection diesel engine. In the test engine, the spray pressure, spray advance, dynamometer load, and turbo pressure of the experimental engine can be changed using an electronic control. The engine does not start before reaching the operating conditions. The engine is ignited by motion through the dynamometer via the computer system. The technical specifications of the experimental engine are given in Table 1.

Table 1. Technical specifications of the experimental engine.

Features	Value
Fuel	Diesel
Engine Timing	Four Stroke
Number of Cylinders	Single Cylinder
Number/Type of Valves	3 (2 Intake–1 Exhaust)/Overhead Valve
Cylinder Volume	1120 cm^3
Cylinder Diameter	106.5 mm
Cylinder Stroke	127 mm
Compression Ratio	16.4/1
Maximum Torque	160 Nm
Maximum Power	50 kW
Maximum Engine Speed	2500 RPM
Maximum In-Cylinder Pressure	190 bar

The data were measured by loading the experimental engine at different load values and three different speeds. For each load value and each fuel, the engine was operated at engine speeds of 1000, 1250, and 1500 RPM. At each speed, the engine was loaded under 25%, 50%, 75%, and 100% loads. Additionally, these tests were performed with the TEG system. In this way, electricity generation by the TEG system was analyzed and the changes in engine performance, exhaust emission, and combustion characteristics were measured and examined.

2.2. Characteristics of Test Fuels

In the study, plant-based biodiesel was purchased from the market and mixed to obtain diesel–biodiesel blends. Table 2 shows the physical and chemical properties of biodiesel and diesel fuel, measured at TUBITAK Marmara Research Center. Biodiesel fuel was mixed with commercial diesel fuel at rates of 0, 10%, 20%, 50%, and 100% by volume. The mixes are coded B0, B10, B20, B50, and B100, respectively.

Table 2. Physical and chemical properties of biodiesel and diesel fuel.

Features	Unit	Biodiesel	Diesel
Density 15 °C	kg/m^3	883.7	829.6
Cetane Number	-	51.3	55.3
Viscosity 40 °C	mm^2/s	4.367	3.215
Flash Point	°C	171.0	59.90
Cold Filter Pluing Point (CFPP)	°C	−2	−16
Water	% (m/m)	0.020	0.006
Iodine Number	g iodine/100 g	109	-
Lower Calorific Value	MJ/kg	37.1	42.7

2.3. Characteristics of Thermoelectric System

The thermoelectric generators, which are of the GM300-126-11-12-HS model of European Thermodynamics Ltd. from Leicestershire, United Kingdom, were electrically connected to each other in series 6 thermo-electric modules and placed on the exhaust pipe.

Six thermoelectric modules, with dimensions of 35 mm × 35 mm × 3.875 mm, were used in this study.

A TEG operates at half the open-circuit voltage (V_{OC}), called the matched load output voltage (V), and half the short circuit current (I_{SC}). The maximum power, called the matched load power output (W), was achieved under these conditions. In the product datasheet, the matched load output voltage was reported as 4 V, and the matched load power output was reported as 3 W at hot and cold side temperature values of T_H = 250 °C and T_C = 50 °C, respectively [28].

After the thermoelectric modules were connected in series, the heatsink block was combined with a copper sheath. The copper sheet used in the packaging was preferred due to its heat transfer coefficient and thermal resistance. The hot surface of the thermoelectric module was assembled with the copper sheath through contact, and the cold surface was assembled via contact with the heatsink block. Since both surfaces are not perfectly planar, a thermal paste with a high thermal conductivity coefficient was applied between them. The experiment aimed to ensure perfect heat transfer by filling the invisible point gaps. The TEG system was connected to the exhaust pipe on the experimental setup with adjustable metal clamps. In order to measure current and voltage values over the connection, a 6 V 4 Ah battery was connected as an electrical load. The charge was controlled with a rectifier circuit, integrated into the electrical supply circuit. The current and voltage values obtained from the TEG system were measured with a multimeter. Figure 2 shows a schematic representation of the cooling circuit specific to the TEG structure included in the exhaust system.

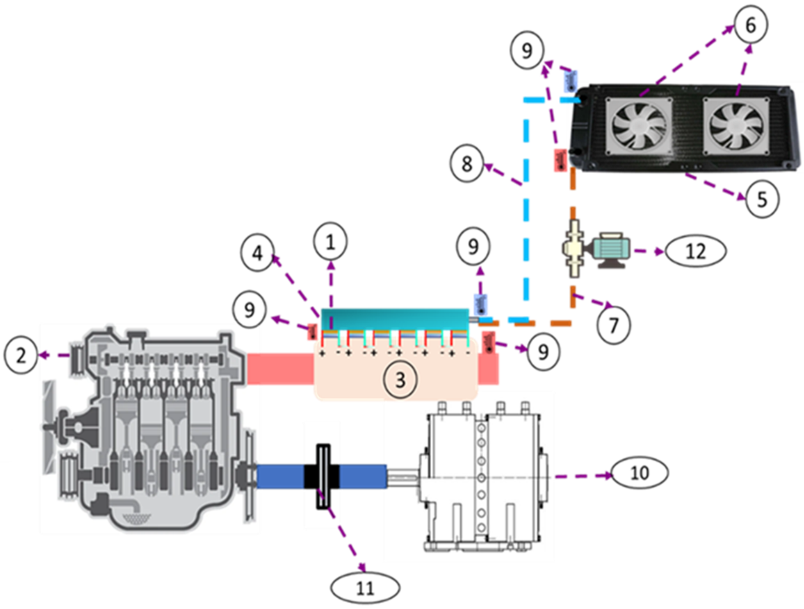

Figure 2. Schematic representation of the cooling circuit (1. Peltier modules; 2. engine; 3. exhaust manifold; 4. cooler block; 5. cooler radiator; 6. fan motor; 7. hot water line; 8. coolant water line; 9. thermometer; 10. Eddy current dyno; 11. clutch; 12. circulation pump).

The Peltier cells used in the study can operate at the highest efficiency when the cold surface is at 30 °C. For this reason, this value was taken into consideration when determining the speed of the DC water pump used as the recirculation pump in the cooling circuit. For this reason, a speed regulation circuit was installed, provided that the temperature measured in the cooling circuit had a maximum of 35 °C.

An aluminum radiator honeycomb was used as the cooling radiator in the cooling circuit. The cooling blocks used in the system were aluminum and manufactured by the aluminum extrusion method, with a high heat transfer capacity and high surface precision, and were 40 × 40 × 12 mm in size. Two 5 V DC fans were positioned on the cooling radiator. The purpose of the fans was to remove the heat on the coolant coming from the

TEG system via forced air convection. Both fans were connected in parallel to each other and energized with an AC-DC voltage reduction adapter.

2.4. Calculation Methods

Cylinder pressure was measured with test equipment and filtered by a digital low-pass filter [29]. In addition, the heat release rate (HRR) was calculated according to the laws of thermodynamics. Break-specific fuel consumption (BSFC), effective efficiency (EE), and energy recovery (ER) were calculated using the data obtained from experimental measurements. BSFC (b_e) is defined as the ratio of the fuel consumption per unit of time to the effective power and calculated by Equation (1) [6].

$$b_e = \frac{m_y \times 3600}{\Delta t \times N_e} \quad (1)$$

where m_y is the amount of fuel, Δt is the unit time, and N_e is the effective power.

The energy released at the end of the combustion in internal combustion engines cannot be completely converted into useful work due to thermal losses. Effective efficiency is calculated by dividing the effective power obtained from the engine by the amount of mass energy consumed per unit of time according to Equation (2) [6].

$$\eta = \frac{3.6 \times 10^6}{H_u \times b_e} \quad (2)$$

where η is an effective efficiency (%) and H_u is the lower calorific value (kJ/kg).

Moreover, the electrical power generation is calculated by Equation (3).

$$P = V \times I \quad (3)$$

where I is the current in amperes, V is the voltage in volts, and P is the electrical power generated in watts.

The Thermoelectric Figure of Merit is dimensionless, and for TEGs to have a high efficiency, the value of zT should be as high as possible [30].

$$zT = \frac{S^2 \sigma T_M}{K_{total}} \quad (4)$$

where S is the Seebeck coefficient ($S = -\Delta V/\Delta T$), σ is the electrical conductivity, T_M is the mean temperature, and K_{total} is the total thermal conductivity. This is the summation of K_l and K_e, which are the thermal conductivities due to the lattice and due to the electrons, respectively.

The efficiency of a TEG can be defined as the ratio of the electrical energy produced (W_{elec}) to the thermal energy entering the hot face (Q_H), and it can be approximated by Equation (5).

$$\eta_{TEG} = \frac{W_{elec}}{Q_H} = \frac{\Delta T}{T_H} \times \frac{\sqrt{1+zT}-1}{\sqrt{1+zT}+\frac{T_C}{T_H}} \quad (5)$$

where zT is typically assessed as the mean hot-side temperature (T_H) and cold-side temperature (T_C) [30].

A TEG can produce its maximum power when it operates at half the open circuit voltage (V_{OC}) and half the short circuit current (I_{SC}), as shown by Equation (6) [30].

$$P_{max} = \frac{1}{2} V_{OC} \times \frac{1}{2} I_{SC} \quad (6)$$

3. Results

The engine was the first run with standard diesel fuel (B0) with no load, and then we checked whether there were any problems in the engine or dynamometer. In the study, data were measured at 1000, 1250, and 1500 RPM for B0, B10, B20, B50, and B100 fuels. In each measurement interval, the engine was operated under 25%, 50%, 75%, and 100% loads. Combustion, performance, exhaust emissions, and energy recovery from waste heat were analyzed with the data obtained in the experimental studies. In addition, a new exhaust design with thermoelectric modules was prepared, and the estimated total energy recovery for this design was calculated using the amount of recovered energy, as measured by the test.

The performance of the diesel engine was evaluated using specific fuel consumption, effective efficiency, and exhaust manifold temperature. In addition, the exhaust emissions of the diesel engine were measured as the amount of carbon dioxide (CO_2), hydrocarbon (HC), and nitrogen oxide (NO_x). In the last section, the electrical power generation and energy recovery were measured using TEGs.

3.1. Cylinder Pressure and Heat Release Rate

The stability and continuity of the average pressure in the cylinder during the operating period is a key factor that ensures performance continuity in internal combustion engines. To compare combustion characteristics, one can examine the pressure and heat dissipation graphs in the cylinder.

The cylinder gas pressure indicates the mixture of air and fuel and combustion ability. By focusing on these factors, the cylinder gas pressure is optimized for the proportion of fuel burnt during the sudden combustion period of burnt gases. This is due to the low thermal energy and other disadvantages of these fuels, which make in-cylinder gas pressure, ignition advance, and flame speed particularly important. Determining the parameters of the optimum ignition advance is crucial when using alternative fuels in diesel engines. The in-cylinder gas pressures were assessed during our tests by operating the engine dynamometer at the standard value, without altering the ignition advance.

The changes in cylinder gas pressures and heat distributions at 75% and 100% engine loads are presented in Figures 3 and 4. Upon examining Figure 3, a general decrease in cylinder gas pressures is observed with an overall increase in the biodiesel ratio in the fuel mixture across all loads. For instance, under 75% engine load, the maximum cylinder gas pressure values, and positions for B0, B20, B40, B60, B80, and B100 fuels are, respectively, 169.28 bar (3° CA) 150.44 bar (4° CA), 158.64 bar (4° CA), 158.88 bar (4° CA), and 158.86 (5° CA). The maximum heat release rates of B0, B10, B20, B50, and B100 fuels were calculated as 98.34 J/°, 97.11 J/°, 102.41 J/°, 97.43 J/°, and 103.56 J/°, respectively.

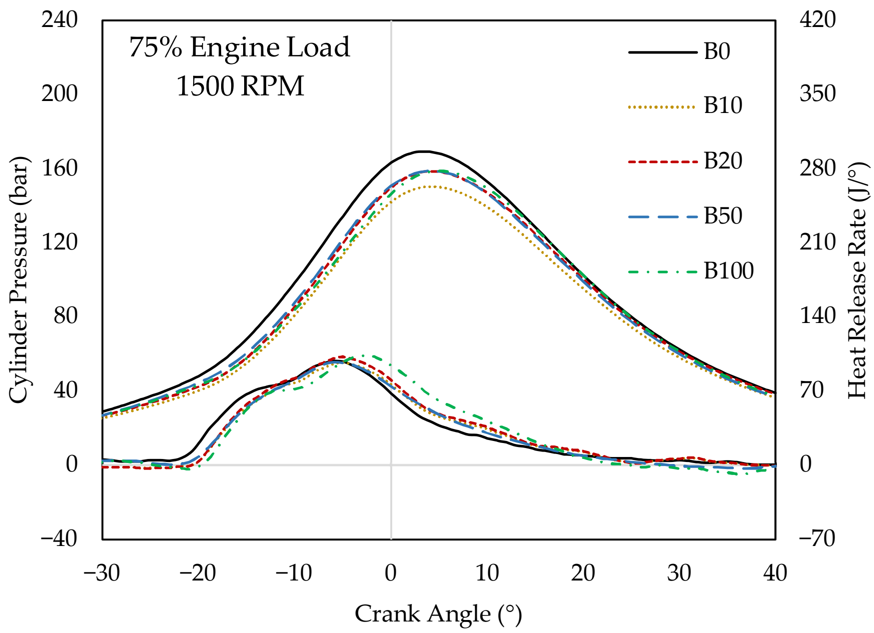

Figure 3. The variation in cylinder pressure and HRR under %75 engine load.

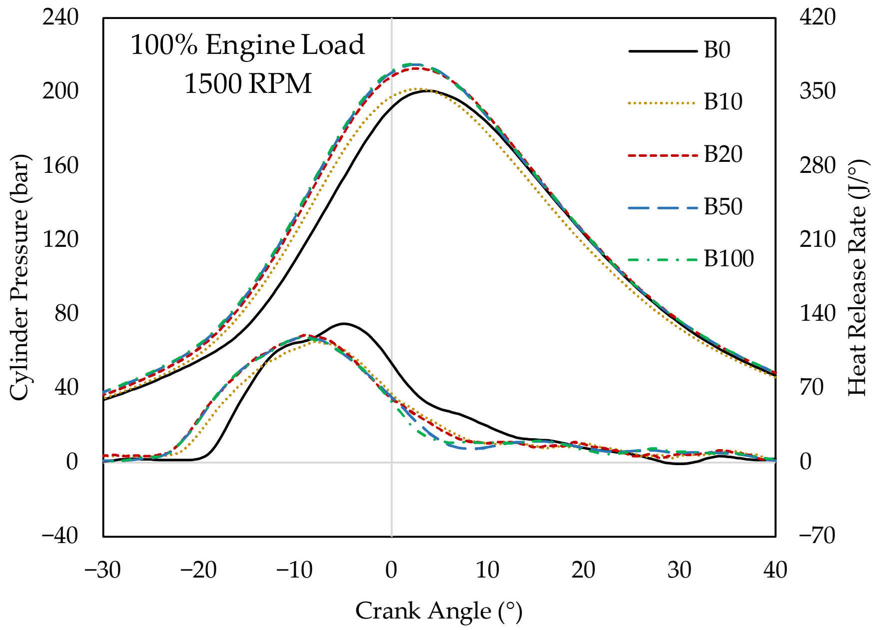

Figure 4. The variation in cylinder pressure and HRR under %100 engine load.

In Figure 3, the heat release rate for fuels containing biodiesel indicates that their heat rise commences later compared to diesel. This delay is attributed to the lower calorific value of biodiesel and its blends, which leads to a prolonged combustion period, resulting in reduced cylinder gas pressures and a reduced heat release rate. Consequently, this shift causes the peak cylinder gas pressure to occur further from the Top Dead Center (TDC). Therefore, the diminished calorific value and peak cylinder gas pressure in biodiesel, in comparison to diesel, adversely impact the heat release rate that is contingent upon these two parameters [31].

The viscosity of the fuel directly affects the size and distribution of fuel droplets when they exit the fuel nozzle. High-viscosity fuels tend to form larger fuel droplets upon exiting the nozzle. This may result in a lower atomization quality and, therefore, a lower combustion efficiency. This situation could be another reason why the pressure and heat distribution rate of biodiesel blends occur later and lower than diesel.

Figure 4 displays the heat distribution graphs of the engine at 1500 RPM and 25%, 50%, 75%, and 100% engine loads under standard spray pressure and advance. For instance, under 100% engine load, the maximum cylinder gas pressure values and positions for B0, B20, B40, B60, B80, and B100 fuels are, respectively, 200.69 (4° CA), 201.74 bar (3° CA), 212.89 bar (3° CA), 214.81 bar (3° CA), and 215.14 (2° CA). The heat release rates of B0, B10, B20, B50, and B100 fuels were calculated with precision as 131.05 J/° 114.19 J/°, 120.48 J/°, 118.97 J/° and 118.41 J/°, respectively. The maximum pressure point shifts forward as the biodiesel ratio increases.

High-viscosity and high-density fuels such as biodiesel tend to form larger fuel droplets. This causes the atomization quality to decrease. High-viscosity biodiesel is more difficult to atomize, which leads to a less homogeneous distribution of fuel in the combustion chamber and, therefore, a decrease in combustion efficiency. However, in order to produce the desired power under maximum load conditions, more biodiesel-blended fuel was injected into the engine. This situation increased the fuel consumption of biodiesel blends. The pressure and heat generated by burning more fuel were higher compared to diesel.

3.2. *Break-Specific Fuel Consumption*

The BSFC is a measure of fuel efficiency. This allows for the fuel efficiency of different engines or fuels to be directly compared. For this aim, the BSFC data calculated for all test conditions and the corresponding graphs are given in Figure 5.

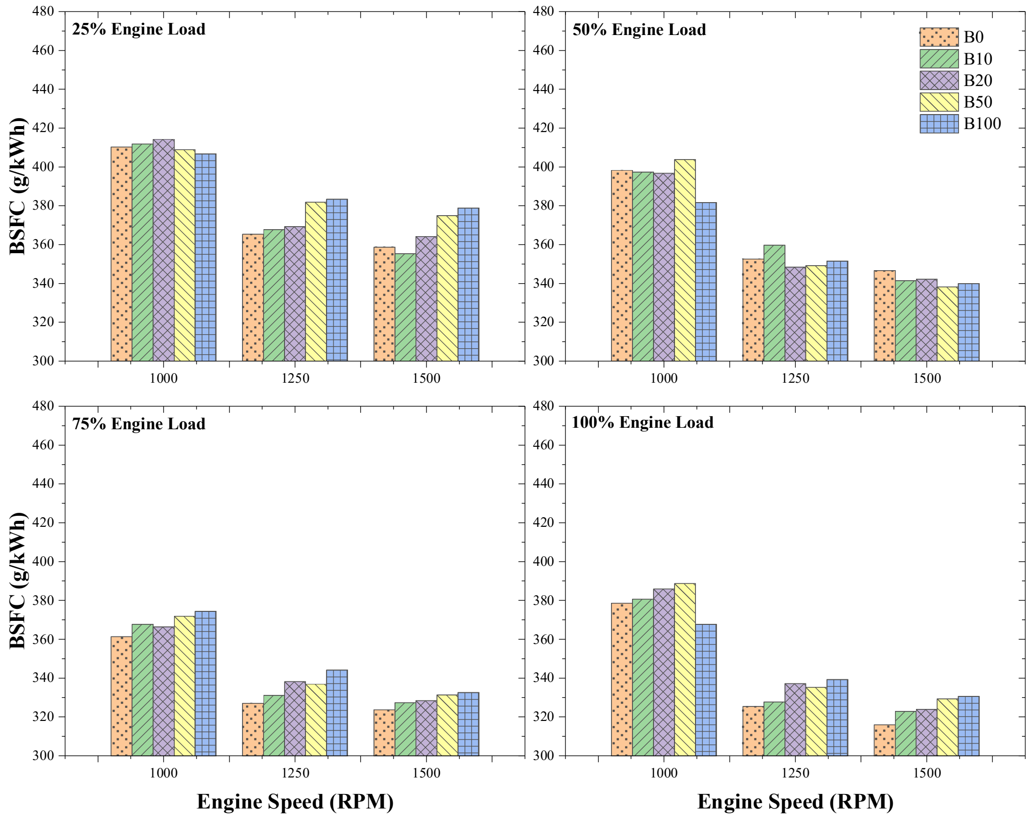

Figure 5. The variation of BSFC.

The BSFC of biodiesel blends was measured to be higher than that of B0 (diesel) at all engine loads and speeds. According to the values, as the percentage of biodiesel in the mixture increases, the specific fuel consumption increases.

The main reason why the specific fuel consumption of biodiesel and its blends is higher than diesel is that the lower calorific value of biodiesel is lower than diesel. To obtain the same amount of energy as diesel, a greater mass of biodiesel fuel must be consumed. In addition, since the density of biodiesel is higher than diesel, the mass of fuel sprayed in equal volumes is higher.

The BSFC decreased with increasing engine load for all fuels. It is known that more fuel is injected into the cylinder per unit of time to increase the engine load. However, the increase rate of the engine load is higher than the increase rate of the injected fuel. For this reason, as the engine load increases, less fuel is consumed. Considering all experimental results, the highest value obtained using B20 fuel was 414.30 g/kWh, at an engine speed of 1000 RPM and under 25% engine load.

In Figure 6, the variation in BSFC is shown to depend on the engine load and speed when using B20. When the test fuel was not changed, the BSFC value decreased according to the increase in engine speed and engine load. According to the consumption values of B20 fuel, 366.40, 338.18, and 328.43 g/kWh values were recorded under the 75% engine load at 1000, 1250, and 1500 RPM, respectively. Another change meant that 364.19, 342.16, 328.43, and 323.89 g/kWh values of B20 were calculated at 1500 RPM under 25% 50%, 75%, and 100% engine loads, respectively.

The variation in BSFC, depending on the engine speed and test fuel at 100% engine load, is shown in Figure 5. When the engine load was not changed, the BSFC value decreased due to the increased air circulation and combustion speed following the increase in engine speed. As the fuel mixture ratio increases, the BSFC value increases. This can be explained by the low viscosity and lower heating value of biodiesel fuel. At a constant engine load of 100%, the BSFC values of B50 fuel at 1000, 1250, and 1500 RPM engine speeds were recorded as 388.70, 335.23, and 329.33 g/kWh, respectively.

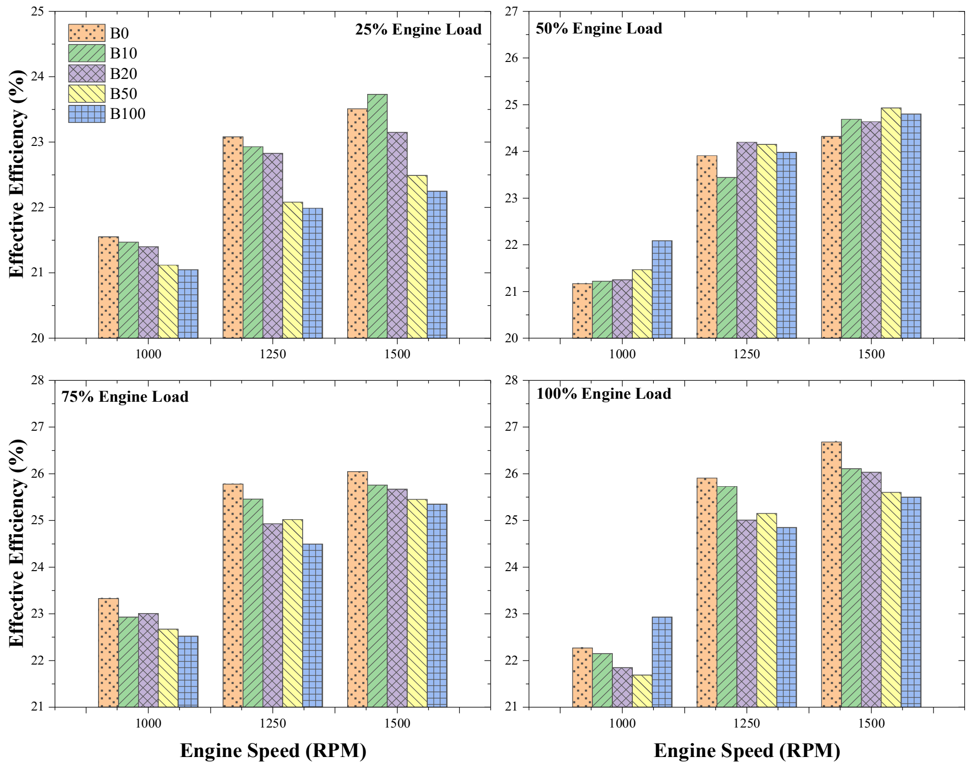

Figure 6. The variation in EE.

3.3. Effective Efficiency

In studies conducted with alternative fuels, effective efficiency is an important parameter when evaluating engine performance. In the tests, as the percentage of biodiesel increased, the effective efficiency generally increased. The reason for this increase in effective efficiency is the increase in the BSFC of fuels using biodiesel, and the decrease in biodiesel compared to diesel occurred because biodiesel consumes more fuel per unit time.

The higher viscosity and density of biodiesel and its lower calorific value compared to diesel are the most important reasons for the decrease in its effective efficiency. The variation in effective efficiency depending on the engine load and test fuel at 1500 RPM is shown in Figure 6. According to the graph, 23.51%, 24.32%, 26.05%, and 26.68% values of B0 were calculated at 1500 RPM under 25% 50%, 75%, and 100% engine loads, respectively. Using B100, 22.25%, 24.80%, 25.35%, and 25.50% values of effective efficiency were calculated at the same engine speed and load.

The fact that the viscosity of biodiesel is higher than the viscosity of diesel causes poor atomization and evaporation. This reduces the effective efficiency of the engine. After evaluating multiple parameters, it was found that the most optimal fuel mixture is B20. The effective efficiency for this fuel mixture increased as engine load and speed increased. According to Figure 6, the highest effective efficiency for B0 is 26.68% at 1500 RPM and 100% load.

According to the effective efficiency values, analyzed under a constant 100% engine load, the effective efficiency increased with the change in speed, while the effective efficiency decreased with the increase in biodiesel ratio. Under that engine load, the effective efficiency was calculated to be 22.93%, 24.85%, and 25.50% for B100 test fuel at 1000, 1250, and 1500 RPM engine speeds, respectively.

3.4. Exhaust Gas Temperature

Exhaust gas temperature (EGT) is an important parameter, as it indicates the combustion temperatures of the fuels used in the tests. The exhaust manifold temperature was determined by measurement with a thermometer in the tests. The variation in EGT according to engine load can be seen in Figure 7. Tests have shown that EGT increases with increasing engine load for all fuels. This rise in EGT is due to the increased amount of fuel that is injected into the cylinder as the engine load increases.

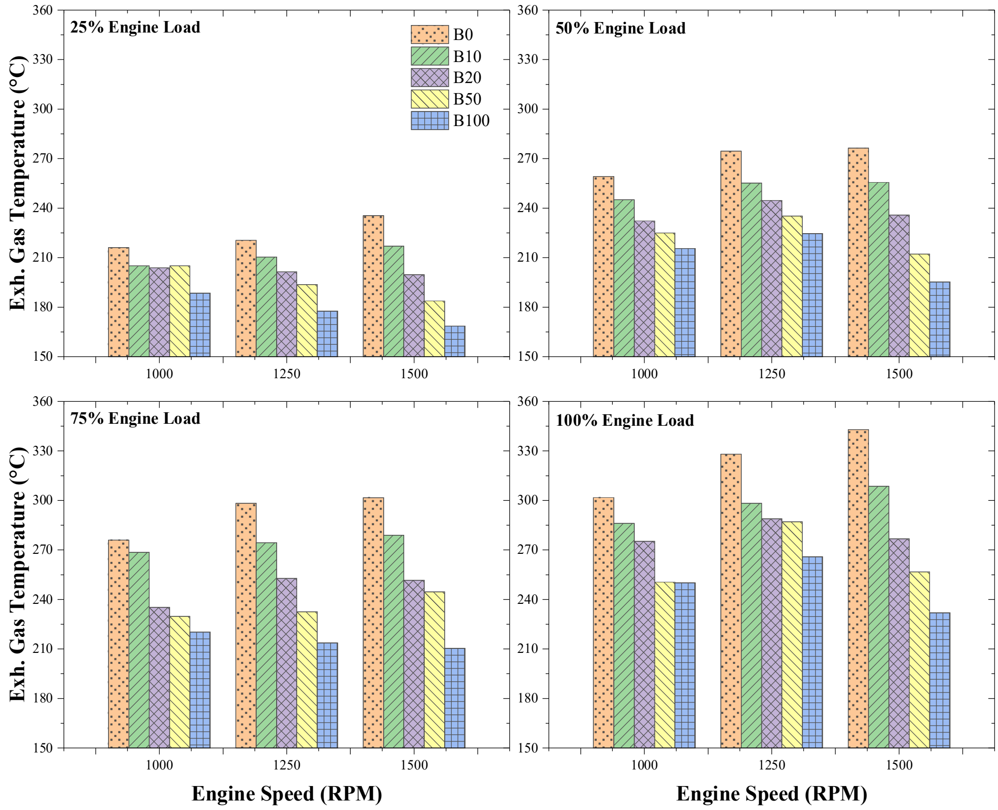

Figure 7. The variation in EGT.

The highest EGT was measured at 342.9 °C at 1500 RPM and under 100% load diesel fuel (B0) usage. At the same engine speed and under the same load, the EGT in the use of B10, B20, B50, and B100 biodiesel blended fuels decreased by 10.00%, 19.31%, 25.14%, and 32.35%, respectively, compared to diesel.

In diesel engines, as the ignition delay is shorter, combustion is completed earlier, and the expansion period is less delayed. As most fuel is consumed before the expansion period, the EGT decreases [32]. In addition, the low energy content of the fuel that is used is also a reason for the low EGT [6]. The decrease observed in EGT with the addition of biodiesel in the tests is because the lower calorific value of biodiesel is lower than that of diesel and most of the fuel is consumed before the expansion period. This situation can be seen in Figure 7.

As engine load increases, more fuel is consumed. Thus, the gas temperature at the end of combustion increases, and this heat is lost through the exhaust. As a result, heat loss through the exhaust manifold increases as engine load increases. At the 1500 RPM engine speed, in the use of B20 fuel, the EGT under 50%, 75%, and 100% loads increased by 18.15%, 26.04%, and 38.61%, respectively, compared to the 25% load state (Figure 7).

When the engine speed increases, the kinetic energy of gases in the combustion chamber rises and it becomes easier for them to collide with each other and enter a chemical reaction. Thus, the combustion improves, and the end-combustion gas temperature and EGT are enhanced. Figure 7 shows the change in EGT at different engine speeds. In the use of B0 and under 100% load, the EGTs at 1000, 1250, and 1500 RPM are measured at 301.85 °C, 328.13 °C, and 342.9 °C, respectively. For the usage of B100, the values of the same conditions are 250.06 °C, 265.93 °C, and 231.96 °C, respectively. These results were obtained because the engine injection parameters were not adjusted according to the optimum combustion conditions of biodiesel.

3.5. CO_2 Emission

Carbon dioxide, among other exhaust products, is an important parameter, as it indicates complete combustion. Additionally, when sufficient oxygen is contained in the combustion chamber, the CO formed during combustion turns into CO_2 [33]. Generally, the oxygen content in biodiesel improves combustion and reduces emissions by providing additional oxygen during combustion. The change in the amount of carbon dioxide measured in tests performed under different engine loads and different speed conditions is shown in Figure 8.

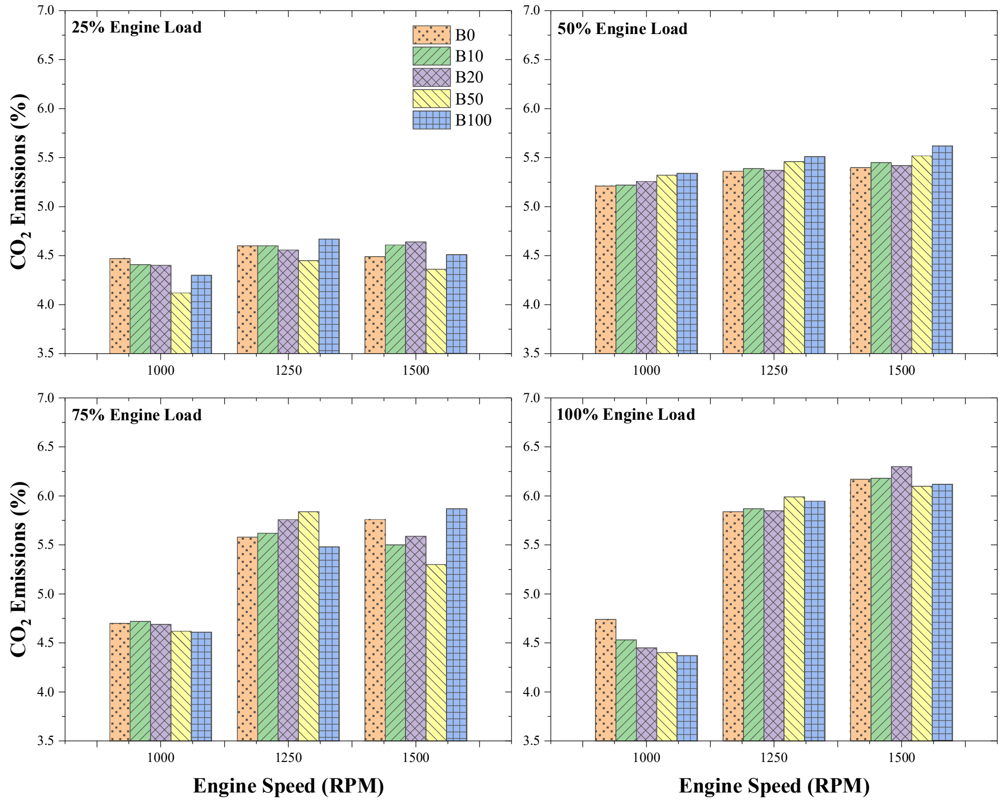

Figure 8. The variation in CO_2 emissions.

Generally, the tests show that CO_2 emissions increase with increasing engine load. BSFC also rises with increasing engine load. Therefore, as the amount of exhaust gas increases, the amount of CO_2 also increases. For this reason, a slight change is observed in the percentage of CO_2 in the exhaust gas.

Additionally, when biodiesel and its blends were used in the tests, it was observed that CO_2 emissions increased slightly compared to diesel at all engine loads. The oxygen contained in biodiesel fuels contributes to CO_2 conversion reactions for biodiesel mixtures. When B0, B10, B20, B50, and B100 are used under 100% engine load and at 1500 RPM, with CO_2 emissions of 6.17%, 6.18%, 6.30%, 6.10%, and 6.12%, respectively.

As the volumetric efficiency decreases as the engine speed increases, the tendency for fuels to burn completely decreases. Since diesel engines are engines that operate with excess air, CO_2 emissions have a nearly horizontal curve at mid-level engine speeds, as seen in Figure 8.

3.6. HC Emission

HC emissions in internal combustion engines primarily arise due to the incomplete combustion of fuel, leaving unburned hydrocarbons to be released into the exhaust. Factors such as cold engine operation, rich fuel mixtures, and inefficient ignition contribute to this phenomenon. While combustion occurs in the engine, no combustion occurs in areas close to the cylinder walls. The main source of HC emissions is the HCs in the flame extinction zone entering the exhaust channel without burning [31]. The HC emissions measured in tests performed at different engine loads and speed conditions are shown in Figure 9. HC emissions in biodiesel and its mixtures are lower than diesel.

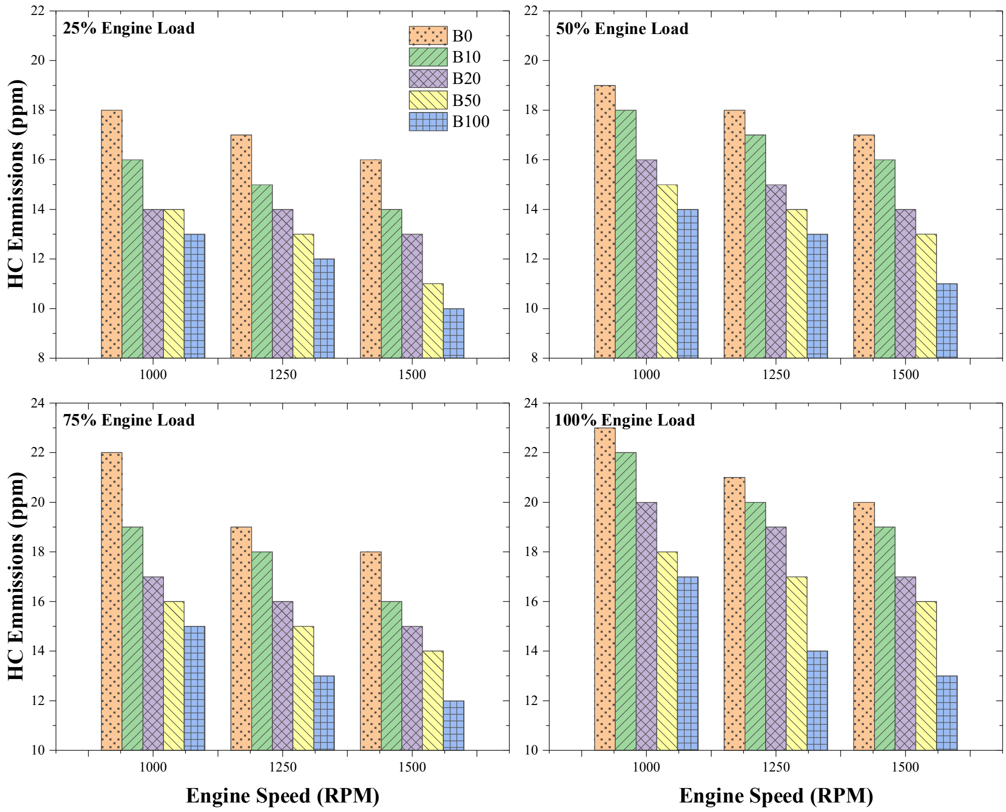

Figure 9. The variation in HC emissions.

It has been observed that HC emissions generally decrease as the percentage of biodiesel in fuel mixtures increases. The oxygen contained in biodiesel increases oxidation rates in rich air–fuel mixture regions with increasing temperatures. Thus, a decrease in HC emissions is observed. When B10, B20, B50, and B100 were used, HC emissions decreased by 5%, 15%, 20%, and 25%, respectively, compared to B0 at a 1500 RPM engine speed and under 100% engine load, as shown in Figure 9. The fact that the HC emissions measured in biodiesel blends are at very low levels supports the literature [34,35]. It is also stated that HC emissions decrease as the cetane number of the fuel increases [36]. The fact that biodiesel has a higher cetane number than diesel supports this situation.

HC emissions increase with increasing engine load. The decreasing in air–fuel ratio with increasing engine load causes the injected fuel to advance to the cylinder walls and further increases the fuel concentration in the core of the fuel jet. Accordingly, in the conducted tests, HC emissions also increase with increases in engine load [37]. Under the engine loads of 25%, 50%, 75%, and 100%, the HC emission values are 13, 14, 15, and 17 ppm, respectively, when using B20 fuels at 1500 RPM.

The reason for the presence of unburned HCs in the combustion products is that the fuel does not reach the ignition temperature, or the fuel will not be oxidized or semi-oxidized due to insufficient oxygen in the environment [38]. The fact that all fuels produce high levels of unburned HC emissions at low engine speeds is due to the fact that specific fuel consumption is at its maximum at these speeds. The values of the HC emissions are 20, 19, and 17 ppm at the engine speeds of 1000, 1250, and 1500 RPM, respectively, using B20 and under 100% engine load (Figure 9).

3.7. NO_x Emissions

During combustion, NO_x emissions occur when oxygen and nitrogen react at high temperatures. The majority of NO_x emissions are NO emissions, a small portion are NO_2 emissions, and the remaining trace amounts are composed of other oxygen–nitrogen combinations. The formation of NO_x emissions is mostly due to the oxygen in the air [39].

The increase in engine load caused in-cylinder temperatures to increase. This situation increased NO_x formation. Since most of the NO_x emissions occurred above 1500 °C, NO_x formation rapidly increases as the temperature increases. The presence of additional oxygen in the environment improves combustion by increasing hydrocarbon oxidation in the combustion chamber during combustion. Thus, improved combustion causes in-cylinder temperatures to rise and NO_x emissions to increase. As a matter of fact, when biodiesel is used, the increasing oxygen level during combustion enhances the maximum gas temperature, thus increasing NO_x formation [31]. When B10, B20, B50, and B100 were used, NO_x emissions increased by 10.98%, 16.74%, 19.80%, and 23.67%, respectively, compared to B0 at a 1500 RPM engine speed and under 100% engine load in Figure 10.

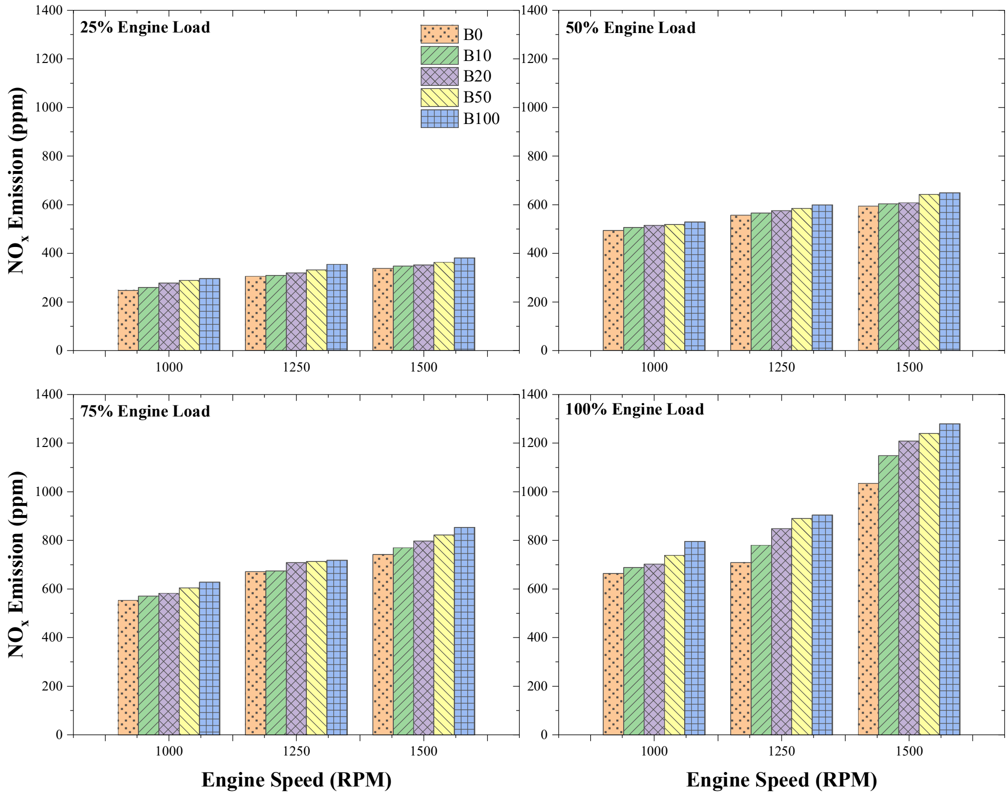

Figure 10. The variation in NO_x emissions.

At high engine speeds, the specific fuel consumption of biodiesel is higher than B0, and the oxygen it contains provides the necessary oxidation in fuel-rich regions, increasing the number of combustion zones. Thus, the number of regions where high ambient temperatures were achieved increased and more nitrogen oxide formation occurred. The values of NO_X emissions for B100 are 796.5, 904.3, and 1280 ppm under 100% engine load and at 1000, 1250, and 1500 RPM, respectively (Figure 10).

3.8. Electric Power Generation via TEG

The TEG system produces an electrical voltage in situations with large temperature differences. The greater the temperature difference, the greater the voltage that is produced. The temperature values at 1500 RPM engine speed and under 25%, 50%, 75%, and 100% loads, measured on the hot and cold surfaces of the TEG system, are given in Table 3.

Table 3. The temperature values on the hot and cold surfaces of the TEG at 1500 RPM.

Fuels	B0		B10		B20		B50		B100	
Load (%)	Surface Temperature (°C)									
	Hot	Cold	Hot	Cold	Hot	Cold	Hot	Cold	Hot	Cold
25	191	61	188	58	187	57	175	56	168	63
50	207	58	196	56	191	54	184	55	177	60
75	221	55	212	54	204	53	203	55	189	57
100	235	55	231	54	210	54	217	55	214	55

In this study, the power generation of the TEG system is calculated by considering the system current and voltage measured under the experimental conditions. During the tests, the voltage was measured using the output of the TEG system, and the current data were measured between the DC/DC converter, which plays an active role in feeding the battery. The measured voltage values at a 1500 RPM engine speed and under 25%, 50%, 75%, and 100% loads are given in Table 4.

Table 4. The voltage values produced by the TEG system at 1500 RPM.

Load (%)	Voltage (V)				
	B0	B10	B20	B50	B100
25	3.03	3.17	3.17	3.05	2.60
50	3.47	3.39	3.44	3.27	2.84
75	3.89	3.80	3.68	3.59	3.24
100	4.14	4.13	3.78	3.83	3.80

The total load resistance of the established circuit was measured as 3.44 Ω. Accordingly, the current value was calculated. In addition, the power was generated by Equation (3). The electrical power graphs obtained for each test fuel at a 1500 RPM engine speed at variable engine loads are shown in Figure 11. In the experiments, it was observed that the electrical power of the TEG system increased as the engine load increased. Exhaust gas temperatures increase with increasing engine load and engine speed. Thus, as the thermal energy transferred to the TEG system increases, the electrical power that is produced also increases.

The electrical power production was highest when diesel fuel was used. The electrical power values for fuel obtained at a 1500 RPM engine speed and under 25%, 50%, 75%, and 100% loads when diesel fuel is used are 2.669 W, 3.500 W, 4.399 W, and 4.982 W, respectively. To obtain more power from the engine, more fuel must be consumed. In this case, more thermal energy is generated, and exhaust gas temperatures increase at high engine loads. In addition, the higher calorific value of diesel fuel than biodiesel increased the gas temperatures at the end of the combustion period. The highest EGT values belong to diesel fuel (Figure 11). Thus, the difference between the hot surface and cold surface of the TEG increased, and the highest electrical power production was achieved. In the tests using biodiesel, the highest electrical power production was obtained with B10 and B20 fuels. Generally, B20 fuel was determined as the optimum fuel mixture according to the experimental results. Additionally, there are studies in the literature on the optimum fuel mixture [1]. When using B20 fuel, which is the most optimum fuel mixture, at a 1500 RPM engine speed and under 25%, 50%, 75%, and 100% loads, the electrical power values that were obtained are 2.921 W, 3.440 W, 3.937 W, and 4.154 W, respectively. The electrical power of B100 fuel under the same experimental conditions is 1.965 W, 2.345 W, 3.052 W, and 4.198 W, respectively. A graph of the change in electrical power production depending on the change in the engine load and biodiesel ratio is given in Figure 11.

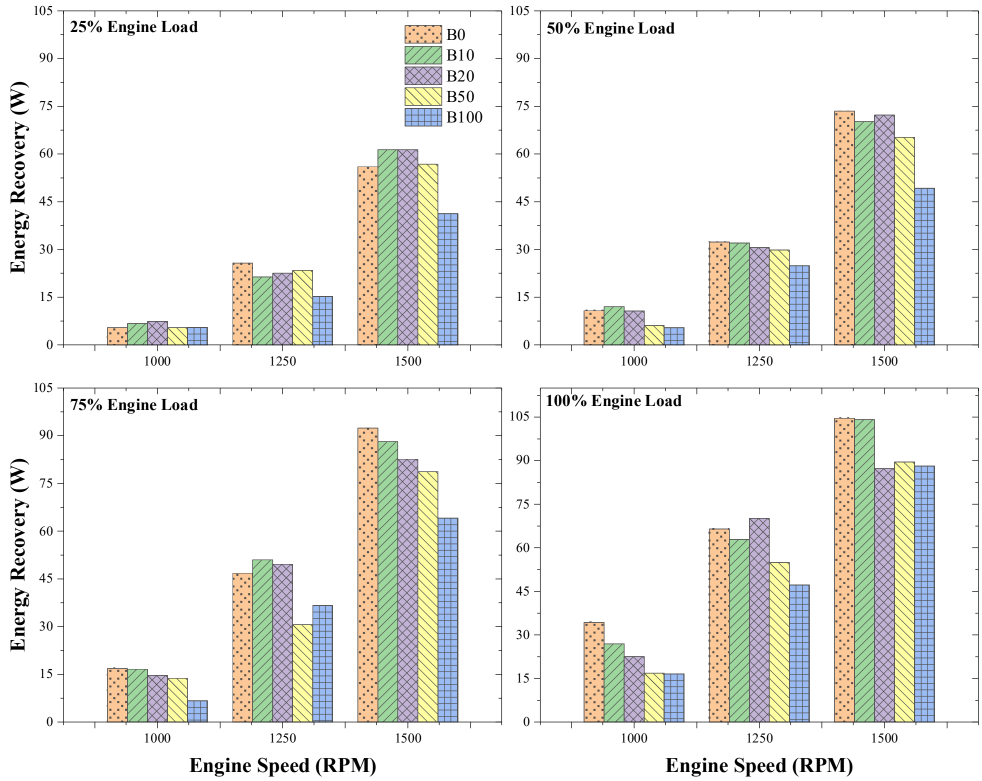

Figure 11. The variation in ER.

According to TEG datasheet, approximately 40% of the maximum power value was produced under 100% load conditions using B20 fuel. Studies similar to these results are available in the literature [18,22,25]. The circuit current caused by the internal resistance of the TEG is given in the catalog as 0.75 A under T_H = 250 °C and T_C = 50 °C conditions [28]. In the experimental study, elements that will create a load on many circuits, such as cooling water circulation, cooling fan, and storage, were included. With these, the current of the circuit increased to around 1.2 A.

In order to increase the engine speed, more fuel was added to the cylinder. Thus, more fuel was burned, producing more thermal energy. According to Figure 11, the most electrical power production was achieved at 1500 RPM and 100% engine load. Under these conditions, the electrical power produced increased by 288% compared to 1000 RPM.

Generally, the electrical power values obtained by increasing the biodiesel ratio in the blended fuel decreased. The reason for this is the decrease in thermal energy as the biodiesel ratio increases. According to Figure 11, the highest electrical power production was achieved from B20 fuel at 1250 RPM engine speed and under 100% engine load conditions. An almost balanced change is observed for 1000 RPM and 1500 RPM.

The TEG efficiency, independent of the entire system was shown to be compatible with the datasheet of TEG. It is stated in the datasheet of TEG that a single TEG module operates with approximately 5–8% efficiency at the specified temperature differences. The Figure of Merit values for p-type and n-type materials are 1.35 and 0.9, respectively [30]. In the calculations, assuming that the zT value is approximately 1, the efficiency of a single TEG module was found to be 7%. These efficiency values are compatible with both the literature and manufacturer data [30].

Many different exhaust designs were proposed in the literature to convert the waste heat into energy in the exhausts of engines using gasoline and diesel [13,18–26]. In this study, based on these experimental studies, a new exhaust design is proposed. This contains 128 modules connected in series. The design is shown in Figure 12. According to this design, 106.28 W was produced for B0 under %100 engine load at 1500 RPM, while 89.56 W of energy was recovered for B100. Under the same conditions, B10 fuel is close to B0 and its value is 105.77 W. These results are similar to studies in the literature [19–24].

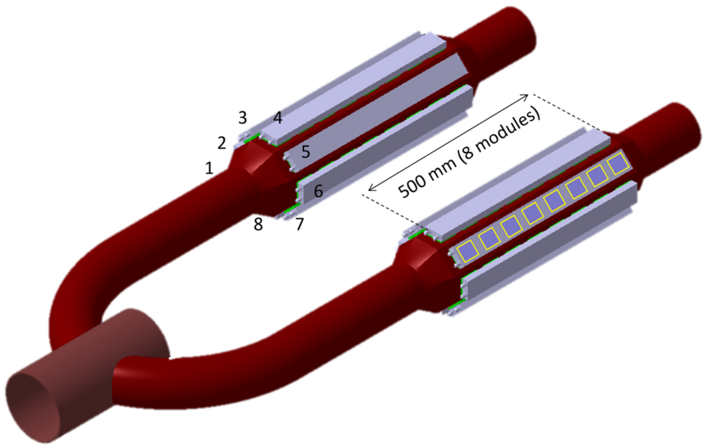

Figure 12. The suggested exhaust design (1–8: TEG groups on surfaces of the octagonal structure).

The exhaust silencers are precisely 500 mm long and feature thermoelectric modules that measure 35 mm × 35 mm. These modules are expertly insulated with thermal paste and spaced 31 mm apart, while being electrically connected to each other in series. Furthermore, each structure on the thermoelectric generator module is equipped with a liquid cooler block, ensuring optimal performance.

4. Conclusions

The fact that oil-derived fuels are expected to decrease within the next 100 years has accelerated the search for alternative sources. Experts suggest that biodiesel could be the closest plant-based alternative to petroleum [40]. Furthermore, biodiesel is considered a viable option for reducing environmental pollution. However, the heat released into the environment through exhaust has a negative impact. Efforts should be made to mitigate this effect. This study's unique contribution is both a new exhaust design with a focus on recovering exhaust heat, and the presentation of a vegetable-based alternative to diesel.

In this study, engine tests were carried out using biodiesel–diesel fuel blends in a diesel engine. During the experiments, a thermoelectric generator designed using thermoelectric modules was used to generate electrical energy by utilizing the waste heat of the engine.

Specific fuel consumption increased with increasing biodiesel content in the experimental fuels. The high viscosity, latent heat of vaporization, and lower calorific value of biodiesel fuel caused an increase in specific fuel consumption compared to diesel under the same experimental conditions. Since the increase in torque is inversely proportional to the specific fuel consumption, the specific fuel consumption tended to decrease with the increase in engine speed and load for all fuels.

Effective efficiency decreased with increasing biodiesel content in the test fuels. This is mainly due to the high viscosity and density of biodiesel and its low heating value. The effective efficiency increased when both engine speed and engine load were increased for the same fuel.

As the biodiesel ratio, engine load, and engine speed increased, NO_x emissions also increased due to the increase in temperature. The start of the spraying of biodiesel is earlier than that of diesel. The ignition delay of biodiesel is less, which causes the controlled combustion phase to be longer in biodiesel than in diesel. Accordingly, NO_x formation increased with increasing biodiesel content due to the high in-cylinder temperature. The highest NO_x emission was obtained under a full load and 1500 RPM for all test fuels.

The exhaust gas temperature showed a change that was directly proportional to the temperature of the manifold to which the TEG system is connected. Due to the increase in biodiesel ratio, the exhaust gas temperatures, and therefore the temperatures between the manifold and the TEG circuit, decreased. Manifold temperature increased with increasing engine speed and engine load. The highest electrical energy produced by the TEG system, consisting of six TEGs in the study, was measured as 4.982 W with B0 fuel, under 100% load, at a 1500 RPM engine speed. In the suggested exhaust design, this is estimated as 106.28 W for the same fuel and under the same conditions. Maximum recovery can be achieved by equipping the entire exhaust manifold with a TEG system. It was concluded that it would be appropriate to design a TEG using 128 serially connected TEGs.

In this case, approximately 100 W energy recovery will be achieved. Although current TEG modules are not very efficient recovery systems because they produce low levels of electrical power, they are promising for the future. It is anticipated that the amount of recovery may be increased with this system depending on the developments in TEG modules in the coming years.

The electrical energy that is obtained can provide an alternative energy source in terms of charging the battery of the vehicle and providing electrical energy to receivers, such as air conditioners, heaters, lamps, etc., in the vehicles.

In addition, researchers are advised to conduct such experiments in gasoline vehicles and make heat recovery measurements. Typically, the research has focused on gasoline engines, since it is stated that higher exhaust temperatures (compared to diesel engines) can be found and a higher percentage of the fuel energy turns into waste heat instead of the mechanical energy needed to move the car compared to diesel engines [15].

Moreover, based on the electrical energy that is produced, this prototype study could be an important source of future generation electric/hybrid cars after design optimization. With some improvements, such as reducing the heat transfer between surfaces, reducing the heat loss on the hot surface, and improving the cooling of the cold surface, the generated electrical energy will be increased. Thus, thermoelectric power generation systems will be an important alternative energy source in the coming years. In addition, it could be more advantageous to use TEG systems in fully efficient heavy vehicles and caravan-style vehicles rather than passenger cars.

Author Contributions: Conceptualization, M.K. and S.E.; methodology M.K. and S.E.; validation, C.S. and S.E; investigation, M.K. and S.E.; writing—original draft preparation, M.K.; writing—review and editing, C.S. and S.E.; visualization, M.K. and S.E.; supervision, C.S. All authors have read and agreed to the published version of the manuscript.

Funding: This research received no external funding.

Data Availability Statement: The data presented in this study are available on request from the corresponding author.

Acknowledgments: I would like to thank TUBITAK, the supporter of science and scientists, and its staff for mobilizing their resources during the experimental stages of the study. This research has not received any financial support from any funding organization in the public, commercial or non-profit sectors.

Conflicts of Interest: The authors declare no conflicts of interest.

References

1. Erdoğan, S.; Balki, M.K.; Aydın, S.; Sayin, C. The best fuel selection with hybrid multiple-criteria decision making approaches in a CI engine fueled with their blends and pure biodiesels produced from different sources. *Renew. Energy* **2019**, *134*, 653–668. [CrossRef]
2. Shabashevich, A.; Richards, N.; Hwang, J.; Erickson, P. Analysis of powertrain design on effective waste heat recovery from conventional and hybrid electric vehicles. *Appl. Energy* **2015**, *157*, 754–761. [CrossRef]
3. Meng, F.; Chen, L.; Feng, Y.; Xiong, B. Thermoelectric generator for industrial gas phase waste heat recovery. *Energy* **2017**, *135*, 83–90. [CrossRef]
4. Kim, T.Y.; Kwak, J.; Kim, B.-w. Application of compact thermoelectric generator to hybrid electric vehicle engine operating under real vehicle operating conditions. *Energy Convers. Manag.* **2019**, *201*, 112–150. [CrossRef]
5. Wang, L.; Song, R.; Zou, H.; Liu, S.; Zhou, L. Study on combustion characteristics of a methanol—Diesel dual-fuel compression ignition engine. *Proc. Inst. Mech. Eng. Part D J. Automob. Eng.* **2008**, *222*, 619–627. [CrossRef]

6. Erdoğan, S.; Balki, M.K.; Aydın, S.; Sayın, C. Performance, emission and combustion characteristic assessment of biodiesels derived from beef bone marrow in a diesel generator. *Energy* **2020**, *207*, 118300. [CrossRef]
7. Triantafyllopoulos, G.; Katsaounis, D.; Karamitros, D.; Ntziachristos, L.; Samaras, Z. Experimental assessment of the potential to decrease diesel NOx emissions beyond minimum requirements for Euro 6 Real Drive Emissions (RDE) compliance. *Sci. Total Environ.* **2018**, *618*, 1400–1407. [CrossRef]
8. Soyler, H. Investigation of the Effect of Biodiesel Produced from Waste Olive by Ultrasonic Method on Performance and Combustion Characteristics of a Diesel Engine. Ph.D. Thesis, Marmara University, Institute of Pure and Applied Sciences, Istanbul, Türkiye, 2023.
9. Leevijit, T.; Prateepchaikul, G. Comparative performance and emissions of IDI-turbo automobile diesel engine operated using degummed, deacidified mixed crude palm oil–diesel blends. *Fuel* **2011**, *90*, 1487–1491. [CrossRef]
10. Sanjid, A.; Masjuki, H.; Kalam, M.; Abedin, M.; Rahman, S.A. Experimental investigation of mustard biodiesel blend properties, performance, exhaust emission and noise in an unmodified diesel engine. *APCBEE Procedia* **2014**, *10*, 149–153. [CrossRef]
11. Niu, Z.; Diao, H.; Yu, S.; Jiao, K.; Du, Q.; Shu, G. Investigation and design optimization of exhaust-based thermoelectric generator system for internal combustion engine. *Energy Convers. Manag.* **2014**, *85*, 85–101. [CrossRef]
12. Liu, C.; Pan, X.; Zheng, X.; Yan, Y.; Li, W. An experimental study of a novel prototype for two-stage thermoelectric generator from vehicle exhaust. *J. Energy Inst.* **2016**, *89*, 271–281. [CrossRef]
13. Orr, B.; Akbarzadeh, A.; Lappas, P. An exhaust heat recovery system utilising thermoelectric generators and heat pipes. *Appl. Therm. Eng.* **2017**, *126*, 1185–1190. [CrossRef]
14. Lan, S.; Yang, Z.; Chen, R.; Stobart, R. A dynamic model for thermoelectric generator applied to vehicle waste heat recovery. *Appl. Energy* **2018**, *210*, 327–338. [CrossRef]
15. Fernández-Yáñez, P.; Armas, O.; Kiwan, R.; Stefanopoulou, A.; Boehman, A. A thermoelectric generator in exhaust systems of spark-ignition and compression-ignition engines. A comparison with an electric turbo-generator. *Appl. Energy* **2018**, *229*, 80–87. [CrossRef]
16. Dincer, I.; Ezzat, M.F. Development an assesssment of a new hybrid vehicle with ammonia and hydrogen. *Appl. Energy* **2018**, *219*, 226–239.
17. Ziolkowski, A. Automotive Thermoelectric Generator impact on the efficiency of a drive system with a combustion engine. In Proceedings of the VII International Congress on Combustion Engines, MATEC Web of Conferences, Poznan, Poland, 27–29 June 2017.
18. Uysal, F. Theoretical and Experimental Investigation of Thermoelectric Generator Application to the Vehicle Exhaust System. Ph.D. Thesis, Karabuk University Graduate School of Natural and Applied Sciences, Karabuk, Türkiye, 2018.
19. Temizer, İ.; Ilkiliç, C.; Öner, C. Dizel Motor Egzoz Sistemi için Termoelektrik Jeneratör Uygulaması ve Akış Analizi. *Afyon Kocatepe Üniversitesi Fen Ve Mühendislik Bilim. Derg.* **2016**, *16*, 431–445.
20. Güneş, S.; Hançer, E. Termoelektrik Modül Kullanarak İçten Yanmalı Bir Otomobilin Egzozundan Atılan Isıdan Enerji Geri Kazanımının Termal Analizi. *Erciyes Üniversitesi Fen Bilim. Enstitüsü Fen Bilim. Derg.* **2017**, *33*, 1–12.
21. Mohammed, S. Development and performance analysis of a TEG system using exhaust recovery for a light diesel vehicle with assessment of fuel economy and emissions. *Appl. Therm. Eng.* **2019**, *147*, 661–674. [CrossRef]
22. Remeli, M.F.; Date, A.; Orr, B.; Ding, L.C.; Singh, B.; Affandi, N.D.N.; Akbarzadeh, A. Experimental investigation of combined heat recovery and power generation using a heat pipe assited thermoelectric generator system. *Energy Convers. Manag.* **2016**, *111*, 147–157. [CrossRef]
23. Hsu, C.T.; Huang, G.Y.; Chu, H.S.; Yu, B.; Yao, D.J. Experiments and simulations on low-temperature waste heat harvesting system by thermoelectric power generators. *Appl. Energy* **2011**, *88*, 1291–1297. [CrossRef]
24. In, B.D.; Kim, H.I.; Son, J.W.; Lee, K.H. The study of a thermoelectric generator with various thermal conditions of exhaust gas from a diesel engine. *Int. J. Heat Mass Transf.* **2015**, *86*, 667–680. [CrossRef]
25. Kim, T.Y.; Negash, A.A.; Cho, G. Waste heat recovery of a diesel engine using a thermoelectric generator equipped with customized thermoelectric modules. *Energy Convers. Manag.* **2016**, *124*, 280–286. [CrossRef]
26. Kim, T.Y.; Negash, A.; Cho, G. Experimental and numerical study of waste heat recovery characteristics of direct contact thermoelectric generator. *Energy Convers. Manag.* **2017**, *140*, 273–280. [CrossRef]
27. Mostafavi, S.A.; Mahmoudi, M. Modeling and fabricating a prototype of a thermoelectric generator system of heat energy recovery from hot exhaust gases and evaluating the effects of important system parameters. *Appl. Therm. Eng.* **2018**, *132*, 624–636. [CrossRef]
28. GM300-126-11-12-HS. Thermoelectric Generator Module. 2024. Available online: https://docs.rs-online.com/fddf/0900766b81715074.pdf (accessed on 30 January 2024).
29. Brown, B. *Combustion Data Acquisition and Analysis, Final Year Project M. Eng. Automotive Engineering*; Department of Aeronautical Loughborough University: Loughborough, UK, 2001.
30. Jouhara, H.; Żabnieńska-Góra, A.; Khordehgah, N.; Doraghi, Q.; Ahmad, L.; Norman, L.; Dai, S. Thermoelectric generator (TEG) technologies and applications. *Int. J.* **2021**, *9*, 100063. [CrossRef]
31. Ozsezen, A.N.; Canakci, M.; Sayin, C. Effects of biodiesel from used frying palm oil on the exhaust emissions of an indirect injection (IDI) diesel engine. *Energy Fuels* **2008**, *22*, 2796–2804. [CrossRef]

32. Aktaş, A.; Sekmen, Y. Biyodizel İle Çalışan Bir Dizel Motorda Yakıt Püskürtme Avansının Performans ve Egzoz Emisyonlarına Etkisi. *Gazi Üniversitesi Mühendislik-Mimar. Fakültesi Derg.* **2008**, *23*, 199–206.
33. Nalgundwar, A.; Paul, B.; Sharma, S.K. Comparison of performance and emissions characteristics of DI CI engine fueled with dual biodiesel blends of palm and jatropha. *Fuel* **2016**, *173*, 172–179. [CrossRef]
34. Kumar, N.; Chauhan, S.R. Performance and emission characteristics of biodiesel from different origins: A review. *Renew. Sustain. Energy Rev.* **2013**, *21*, 633–658. [CrossRef]
35. Basha, S.A.; Gopal, K.R.; Jebaraj, S. A review on biodiesel production, combustion, emissions and performance. *Renew. Sustain. Energy Rev.* **2009**, *13*, 1628–1634. [CrossRef]
36. Wu, F.; Wang, J.; Chen, W.; Shuai, S. A study on emission performance of a diesel engine fueled with five typical methyl ester biodiesels. *Atmos. Environ.* **2009**, *43*, 1481–1485. [CrossRef]
37. Doğan, O.; Celik, M.B.; Özdalyan, B. The effect of tire derived fuel/diesel fuel blends utilization on diesel engine performance and emissions. *Fuel* **2012**, *95*, 340–346. [CrossRef]
38. Ağbulut, Ü.; Sarıdemir, S.; Albayrak, S. Experimental investigation of combustion, performance and emission characteristics of a diesel engine fuelled with diesel–biodiesel–alcohol blends. *J. Braz. Soc. Mech. Sci. Eng.* **2019**, *41*, 389. [CrossRef]
39. Alptekin, E. Emission, injection and combustion characteristics of biodiesel and oxygenated fuel blends in a common rail diesel engine. *Energy* **2017**, *119*, 44–52. [CrossRef]
40. Eremeeva, A.M.; Ilyushin, Y.V. Automation of the control system for drying grain crops of the technological process for obtaining biodiesel fuels. *Sci. Rep.* **2023**, *13*, 14956. [CrossRef]